Masao Kuroda. International Journal of Engineering Research and Applications
www.ijera.com
ISSN: 2248-9622, Vol. 15, Issue 8, August 2025, pp 11-19

RESEARCH ARTICLE OPEN ACCESS

Optimization of Successive Operations of Filtration and Backwash based on Residual Deposits

Masao Kuroda*
**(Professor emeritus of Gunma University, 4-2 Aramakicho, Maebashi, Gunma 371-8510, Japan)*

ABSTRACT
Experimental results from successive filter runs with fluidized backwash were analyzed using the phenomenological model based on quantitative results related to filtration and backwash period. Particular emphasis was placed on the effect of the filtration/backwash interaction on the characteristics of the successive operations of filtration and backwash. Conventional backwash duration is likely to result in over-efficient cleaning. In successive operations of filtration and backwash, there is a threshold of residual deposits to eliminate the filter ripening stage, which is affected by the characteristics of filter beds. The two-stage backwash method, consisting of a first stage backwash and a second stage backwash following the first stage with specific conditions of backwash flow rate and backwash duration is useful for controlling the filter ripening stage. By appropriately decreasing the first stage backwash duration, the increased residual deposits will ensure that the filter ripening stage is eliminated. The operating conditions predicted based on residual deposits may be applied not only for controlling filter ripening, but also for assessing the effectiveness of the filtration operation. The amount of residual deposits would be a relevant basic condition for an optimum filtration operation and the time to peak concentration of the backwash effluent would be an indicator of effective backwash duration.
Keywords - backwashing, filtration, filter ripening, residual deposits, mathematical modelling

---

Date of Submission: 01-08-2025 Date of acceptance: 11-08-2025

I. INTRODUCTION

In rapid filtration, backwashing of the filter media is a crucial step for an effective filtration process, as the filtration operation is repeated multiple times to treat the raw water. Inadequate cleaning of the filter during backwashing will inevitably deteriorate the filter bed, which may ultimately affect filter performance. The majority of previous studies have focused on filtration and backwashing characteristics [1-6]. The backwash condition has been studied in relation to the bed expansion ratio, and the backwash condition has been determined by the backwash flow rate corresponding to the effective bed expansion ratio. However, conventional backwash conditions do not always indicate an optimum filtration condition. Filter ripening, the period of degraded filter effluent quality immediately following backwashing, as well as the accumulation of dirt aggregates, are well known problems in water treatment [7-9]. Filter-to-waste is commonly used to eliminate the degraded quality filter effluent in many water treatment facilities, which results in a large amount of filter effluent discharge. Basically, filter ripening is caused by the interaction between filtration and backwashing, resulting from a sequence of filtration and backwash cycles. Colton et al. showed that both a long backwash duration, resulting in over-efficient cleaning, and a very short backwash duration, resulting in inefficient cleaning, cause filter ripening [9]. Amburgey showed that successive operations of filtration and backwash with the two-stage backwash method (ETSW backwashing procedure) would maintain an effective mature state in the filter bed [10]. These results indicate that a certain amount of deposit remaining in the filter after backwashing can be beneficial for subsequent filtration runs, and filter ripening would depend on the amount of deposits retained in the filter bed. This also suggests that there is a threshold of residual deposits to eliminate the filter ripening. However, there is little fundamental research into residual deposits based on successive operations of filtration and backwash [11] and few models available for analysis of combined filtration and backwash [12].

This paper presents experimental results obtained from successive filter runs with fluidized backwashing, producing a phenomenological model based on quantitative results related to filtration and backwash period; the results are related to filtration and backwashing and the effect of the deposits remaining after backwash and the backwash duration on filter ripening.

II. MATERIALS AND METHODS

2.1 Sample preparation and experimental conditions

Raw water was prepared by adding kaolin clay powder (Kanayakousan, Clay No.15 2600kg/m^3) into tap water with the concentration of 3 mg/L. The coagulant polyaluminium chloride (PACl) (PAC 6010 liquid, basicity 55-65%,10-11% Al_2O_3, specific gravity 1.2 (Taimei Chemicals Co., Ltd. Tokyo Japan)) in an average dose of 20 m/gL was injected into the raw water line at a set place located just before the static mixer, and the raw water was then directed to the filter.

Particles loaded into the filter during each filter run were kaolin clay, K and PACl floc, P. These were calculated as follows. P was 2 moles of aluminum hydrate ($Al(OH)_3$) produced from 1 mole of aluminum oxide (Al_2O_3). K and P were calculated using the equations $K=QC_k$ and $P=0.153\alpha QC_p$ respectively (Q: raw water (m^3), C_k: turbidity (kg/m^3), α: Al_2O_3 content (-), C_p: PACl dose (kg/m^3)).

The filtration rate was 140 m/day, and the filtration operation was ended when the head loss reached 20kP. The backwash conditions were set based on the operation data obtained from conventional water treatment facilities in the Kanto area. At the end of filter run, the filter was backwashed with pre-determined backwash rates (36 m/h or 54 m/h) and backwash duration (216 seconds or 161 seconds) using tap water, the backwashed filter was then used for the next filter run. The backwash effluent was collected in 200 liters plastic tanks. For the experiments, raw water temperature and backwash water temperature varied between 17 and 18 ℃.

Filtration rate, temperature and head loss profile were recorded during the course of each run. Grab samples of the raw water and filtrate were collected at various intervals and analyzed for turbidity. The total volume of water filtered during each run was calculated from the flow rate measurements. Once backwash was complete, the effluent volume was measured. Samples of the mixed effluent were collected for turbidity and suspended solids measurements. The turbidity measurement was carried out using a turbidity meter (Turbidity meter WA 6000, Nippon Denshoku Industries Co., Ltd. Tokyo Japan), and the suspended solids measurement was carried out based on JISK1020. After discharging the content, the plastic tank was washed fully using clean water. The mass of solids of the backwash effluent determined from the suspended solids concentration was termed mass dislodged, MD, and was expressed in units of kg mass of solids per m^2 of cross-sectional filter area. The mass of residual deposits, also expressed in units of kg mass of solids per m^2 of cross-sectional filter area, was termed MR.

A video camera (Sony HDR-CX680) was set up on a tripod to one side of the filter and taping was done in order to record the expansion and the disintegration of the filter bed, etc.

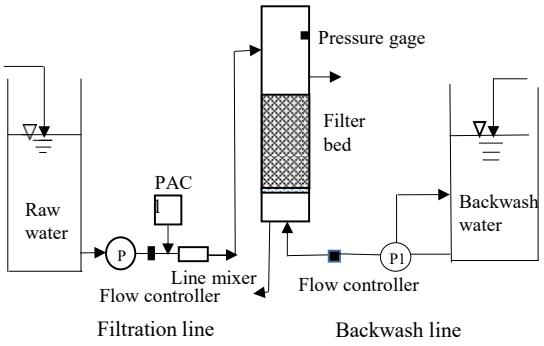

Fig.1 Schematic diagram of the experimental apparatus

2.2 Experimental setup of filter

A schematic diagram of the experimental apparatus is shown in Fig.1. The filtration column is a transparent polyvinyl chloride pipe with a diameter of 200 mm and a total height of 1600 mm; a scale for measuring the filter bed height was attached to the surface of the filter column. The filter media were silica sand (effective size of 0.6 mm, d_{ps} and uniformity coefficient of 1.5) and anthracite (effective size of 1.2 mm, d_{pa} and uniformity coefficient of 1.5) and the specified bed height was 600 mm consisting of 200mm anthracite and 400 mm silica sand. The filter media grains were supported on a porous resin plate with a porosity of about 33% and a pore diameter of 1 mm. The raw water line consisted of a raw water tank, a polyaluminium chloride reservoir, a pump, a static mixer, a flow controller and a pressure gauge. The backwash line consisted of a backwash water tank, a pump and a flow controller.

III. RESULTS AND DISCUSSION

3.1 Cumulative mass retained and mass dislodged in successive filtration and backwash cycles

The chain lines in Fig. 2 show MR and MD in individual cycle runs as a function of the number of cycles. The backwash flow rate was 36m/h. MR was obtained by subtracting MD from the sum of K and P, discussed previously, since the filtrate turbidity was 0.05 mg/L or less, and little sludge was observed in the filtrate.

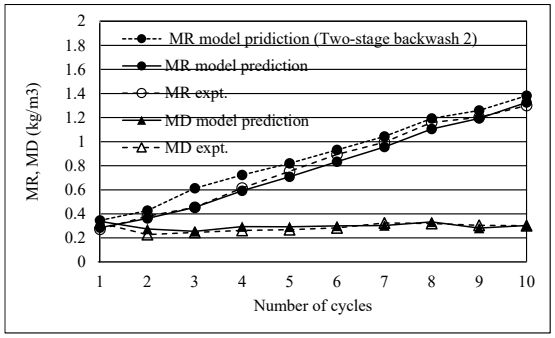

Fig.2 Model prediction and experimental results for the cumulative mass retained after backwash, MR and the dislodged mass, MD (backwash flow rate 36 m/h, backwash duration 216 sec).
Two-stage backwash 2 (backwash duration: 1st stage 75sec, 2nd stage 206 sec).

MD showed a small overall increase, and MR showed a steady increase with the number of cycles. This result indicates that particles deposited during a particular filter run were not removed during the backwash at the end of that particular run, and it became increasingly less likely that they were removed during subsequent backwashes.

The ratio of deposits remaining after backwashing to deposits remaining before backwashing increased with the number of cycles, asymptotically approaching a maximum value.

3.2 Time concentration changes in the filtration effluents

The chain line in Fig.3 shows a typical filter effluent concentration profile in the second cycle of successive operations of filtration and backwash. The backwash flow rate was 36m/h. It shows that there is a short lag before the turbidity peak followed by a quick decay and a gradual decrease in turbidity.

The literature suggests that there are two broad working stages in rapid filtration [6,10,17], the filter ripening stage that filter effluent quality is degraded and the operable stage. In the filter ripening stage particles begin to deposit onto the filter media grains which are clean. The mass of residual deposits on the filter media grains increases with time, and the deposits coat the filter media grains. Removal of deposited particles does not occur during this stage [13]. When the filter ripening duration was taken as the time required for the effluent concentration to fall below 0.1 mg/L, the filter ripening duration was approximately 25 minutes. The filter ripening duration is usually between 20 and 120 minutes, depending on various conditions such as influent turbidity, flow rate, filter media size and backwashing [14]. In the operable stage particles are deposited on top of previously deposited particles and both deposition of solids and re-entrainment by flow occur in parallel [13,15-17].

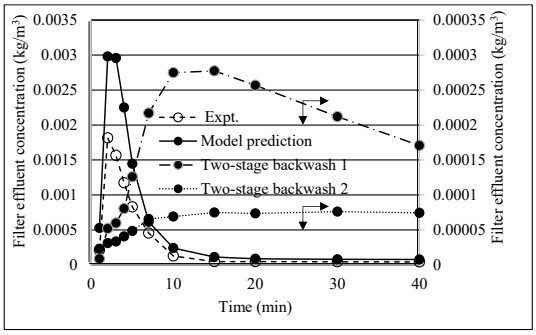

Fig.3 Filtration effluent concentration profile in the second cycle of successive operations of filtration and backwash. (backwash flow rate 36 m/h, backwash duration 216 sec).
Two-stage backwash 1 (backwash duration:1st stage 216sec, 2nd stage 206 sec)
Two-stage backwash 2 (backwash duration:1st stage 75sec, 2nd stage 206 sec)

For each filter ripening to operable stage transition, a corresponding transition values of deposits was assumed as follows; the transition from the filter ripening stage to the operable stage takes place when the deposit reaches q_1 (kg/m^3) which corresponds to the total mass of layer formed on the filter grains [13,16,17]. Since the volume of residual deposits that can be retained by the filter bed is finite not only because of the porosity of the filter bed but also because of turbidity breakthrough, a saturation stage is eventually reached when the mass of residual deposits reaches its maximum feasible value, q_2 (kg/m^3).

3.3 Time concentration changes in backwash effluents

The chain line in Fig.4 shows a typical backwash effluent concentration profile in the second cycle of successive operations of filtration and backwash. The backwash flow rate was 54m/h. Experimental data show an initial lag and turbidity peak followed by a quick decay and a gradual decrease in turbidity. The discharge of residual deposits was divided into three stages; a lag stage, a violent discharge stage where the turbidity peak and a quick decay appear, and a steady discharge stage of gradual decrease in turbidity.

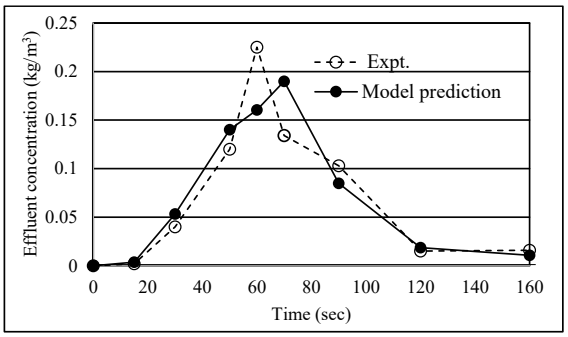

Fig.4 Backwash effluent concentration profile in the second cycle of successive operations of filtration and backwash (backwash flow rate 54 m/h , backwash duration 161 sec).

The backwashing period was classified into three stages based on observed fluidization states. They were a mostly fixed stage, a violent agitation stage and a stabilized stage respectively. Consideration of the backwash effluent concentration profile together with the observations by video photography have greatly enhanced our understanding of the mechanism behind backwashing. The mostly fixed stage corresponds to the lag stage. However, at this stage the top layer of the filter bed was clogged with deposits, and began to tilt and buckle. The duration was approximately five to twenty seconds, depending on the backwash flow rate. The violent agitation stage corresponds to the violent discharge stage, in which the top layer of the filter bed and the freeboard are violently agitated for several tens of seconds by the backwash water instantaneously ejected out the filter bed (backwash water jet). The higher the backwash flow rate, the greater the agitation by the backwash water jet. This stage was further divided into a quick ejection stage and a turbulence stage. The quick ejection stage corresponds to the initial stage of the violent discharge stage, and the filter media grains of the top layer of the filter bed are flushed out of the filter bed and are violently agitated in the freeboard with the backwash water jet. The duration was approximately five to ten seconds, depending on the backwash flow rate. The turbulence stage is a transitional stage to the stabilized stage that follows the quick ejection stage, during which effluent concentration decreases quickly. The stabilized stage corresponds to the steady discharge stage.

Fig.4 shows that approximately 65 % of the total mass removed by the backwash is carried away at the beginning of the turbulence stage. This suggests that the violent disturbance of the backwash water jet will rub the residual deposits off the filter media particles.

3.4 Modeling and simulation

3.4.1 The kinetics of particle deposition in filtration

The particle removal process can be expressed by the following kinetic equation, which combines the Iwasaki equation [18] and the material balance equation.

$$\frac{dq}{dt} = \lambda C u \qquad (1)$$

where C is the particle concentration (kg/m^3), u is the superficial velocity (m/h), t is the time (h), q is the deposits defined as the amount of material deposited per unit volume of the filter (kg/m^3), and λ is the filtration coefficient (1/m). λ depends on the specific surface area and porosity of the filter bed which are altered by the accumulation of deposits [13,16,19]. λ is usually expressed as a function of q, and the form of function has been studied by many researchers [2,6,20]. In this study the effect of q on λ was expressed based on the discussion in the previous section as follows. Since q increases irreversibly in the filter ripening stage, λ was expressed by $K_1(1 + q/q_1)^{lm}$. On the other hand, q increases or decreases because both the attachment of solids and re-entrainment by the flow occur in parallel in the operable stage, so λ was expressed by $K_2(1 + q/q_2)^{lm}(1 - q/q_2)^{ln}$. K_1 and K_2 are the respective coefficients (1/m) and l_m and l_n are the respective exponents which are obtained from experiments.

3.4.2 The kinetics of particle detachment in backwashing

The particle detachment rate was assumed to be proportional to the deposits as expressed in the following equation.

$$\frac{dq}{dt} = -D_k q \qquad (2)$$

where D_k is the detachment coefficient (1/h). The value of D_k varies with the fluidized state of the filter bed. The detachment rate would increase with the increasing freshly deposited solids. However, it would decrease with the increase in aged deposits produced by successive cycle runs, as the deposits appear to become more difficult to remove the longer they remain in the filter [11]. The effect of q on D_k was expressed by $D_k(1 - q/q_b)^{l_l}$. q_b (kg/m^3) is the deposit retained in the filter and l_l is the exponent obtained from experiments.

Table 1 Governing equations

Filtration process	
Freeboar	
$\frac{\partial C}{\partial t} = -u\frac{\partial C}{\partial x} + D\frac{\partial}{\partial x}\left(\frac{\partial C}{\partial x}\right)$	(3)
I.C. t=0 C=g(x)	(4-1)
B.C. x=0 C=C_0 x=L C=C_L	(4-2)
Filter layer	
$\frac{\partial \varepsilon C}{\partial t} = -u\frac{\partial C}{\partial x} + D\frac{\partial}{\partial x}\left(\frac{\partial C}{\partial x}\right) - \frac{dq}{dt}$	(5)
$\frac{dq}{dt} = \lambda C u$	(6)
Anthracite layer λ	
1st stage $\lambda_{1a}=K_{1a}(1+\frac{q}{q_{1a}})^{lm}$ $0 < q \leqq q_{1a}$	(7)
2nd stage $\lambda_{2a}=K_{2a}\left(1-\frac{q}{q_{2a}}\right)^{ln}\left(1+\frac{q}{q_{2a}}\right)^{lm}$ $q_{1a} < q \leqq q_{2a}$	(8)
Silica sand layer λ	
1st stage $\lambda_{1s} = K_{1s}\left(1+\frac{q}{q_{1s}}\right)^{lm}$ $0 < q \leqq q_{1s}$	(9)
2nd stage $\lambda_{2s}=K_{2s}\left(1-\frac{q}{q_{2s}}\right)^{ln}\left(1+\frac{q}{q_{2s}}\right)^{lm}$ $q_{1s} < q \leqq q_{2s}$	(10)
I.C. t=0 C=g'(x) q=r'(x)	(11-1)
B.C. x=0 C=C_L x=L $\frac{\partial C}{\partial x} = 0$	(11-2)
Backwash process	
Filter layer	
$\frac{\partial \varepsilon C_b}{\partial t} = -u\frac{\partial C_b}{\partial x} + D_b\frac{\partial}{\partial x}\left(\frac{\partial C_b}{\partial x}\right) - \frac{dq}{dt}$	(12)
Anthracite layer	
$\frac{dq}{dt} = D_{kai}(1-\frac{q}{q_{2a}})^{l_l} q$	(13)
Silica sand layer	
$\frac{dq}{dt} = D_{ksi}(1-\frac{q}{q_{2s}})^{ll} q$	(14)
I.C. t=0 C_b=g(x) q=r(x)	(15-1)
B.C. x=0 C_b=0, x=L $C_b = C_{bL}+D_b\frac{\partial C_b}{\partial x}$	(15-2)
Freeboard	
$\frac{\partial C_b}{\partial t} = -u\frac{\partial C_b}{\partial x} + D_b\frac{\partial}{\partial x}\left(\frac{\partial C_b}{\partial x}\right)$	(16)
I.C. $t = 0$ $C_b = g''(x)$	(17-1)
B.C. x=0 C=C_L x=L $\frac{\partial C}{\partial x} = 0$	(17-2)

The governing equations for the sequence of filtration and backwash cycles, Eq. (3) to Eq. (17), are given in Table 1. In Table 1 the subscripts 1, 2 indicate the filter ripening and operable stages, and the subscripts s, a indicate the sand and anthracite filter beds, respectively.

3.4.3 Numerical solution of the governing equations

The governing equations were solved numerically by using the finite difference. For this purpose, the equations were made dimensionless using the following definitions: $y = C/C_0$, $z = x/L$, $\sigma = q/C_0$, $\theta = (u/L)t$. An explicit algorithm was used for the numerical solution. For stability reasons, a backward-forward finite-difference scheme was chosen. The finite length was divided into 60 equal grid steps.

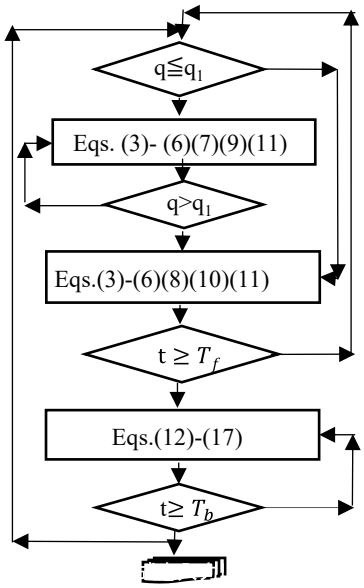

Fig.5 Diagram simulating of the sequence of filtration and backwash cycles

The concentration profile of detached particles in the freeboard cannot be simply estimated, since particles are instantaneously ejected to the freeboard from the filter bed at the beginning of backwash. In this paper, based on the observations from the video photography, the ejected particles were assumed to mix instantaneously during the quick ejection stage. Therefore, the concentration of particles in the freeboard was expressed in terms of the mean

concentration of particles by mass, which was the total mass of solids remained in the freeboard and deposits rubbed out the filter bed divided by the total volume of the freeboard and the top layer of the filter bed. The thickness of the top layer of filter bed flushed by the backwash water jet varied in the range of approximately 5 to 10 cm.

The simulation of the combined filtration and backwash model is shown in Fig. 5. In Fig.5 T_f (h) and T_b (h) are the filtration and backwash times, respectively. Simulation outputs from the filtration model include the outlet concentrations and the deposit concentrations. The deposits and suspended solids concentrations along the filter at the end of the filtration run are used as the initial concentration for the simulation in the backwash model. The backwash model simulation will provide the data on deposits, suspended solid concentrations retained in the filter and effluent concentrations with backwash time. After the first cycle run, the deposits and suspended solids remained in the filter at the end of each backwash simulation will be used as the initial condition for the simulation on the filtration model for the next filter run.

As shown in Table 1, formulation of the problems requires the determination of a number of quantities, including D, K, q and so on. The values of these parameters for the sand filter bed are assigned based on the literature. The values of the hydrodynamic dispersion coefficient in the filtration model, D (m^2/h), were estimated from the literature [21]. In the backwash model the fluidized stage was divided into three stages discussed in the previous section. The values of the hydrodynamic dispersion coefficient for the mostly fixed stage, D_{bFs}, D_{bFa}, D_{bFf}, and the values of the hydrodynamic dispersion coefficient in the stabilized stage, D_{bSs}, D_{bSa}, D_{bFf}, were respectively estimated based on the literature [21,22]. The values of the hydrodynamic dispersion coefficient in the quick ejection stage, D_{bRs}, D_{bRa}, D_{bRf}, were respectively determined based on experimental results. The values of the hydrodynamic dispersion coefficient in the turbulent stage, D_{bTs}, D_{bTa}, D_{bTf}, were respectively determined according to the stabilized stage. The subscript i in Eq. (13) represents each fluidized sate of the filter bed; the subscripts F, R, T, S indicate the fixed, quick ejection, turbulence and stabilized stages, respectively, and the subscripts s, a, f indicate the sand and anthracite filter beds and the freeboard, respectively. The values of other parameters were estimated in the literature as follows [17]; K_1 and K_2 are 0.8 to 3.1 1/m and 6 to 30 1/m respectively, q_1 and q_2 are 0.1 to 0.5 kg/m^3 and 9.5 to 30 kg/m^3 respectively. It is quite difficult to evaluate the threshold, q_1, in the absence of direct experimental data. In the present simulation the values of these parameters were set as follows; q_1 was 0.12 kg/m^3, q_2 was 10.1 kg/m^3. q_2 was the mass of residual deposit measured after the cycle number of 10. q_b was determined as follows; q_{bs} and q_{ba} were q_{2s} and q_{2a} respectively. The subscripts, s and a indicate the sand and anthracite filter beds. Based on the literature [23], the values of ll, lm and ln were set to 0.6, 2.1 and 1.0, respectively, which appeared in the experimental results.

Table 2 Parameters for the anthracite bed

$$K_{1a} = K_{1s}\, dps(1-\varepsilon_{a0})/dpa(1-\varepsilon_{s0}) \quad (18)$$

$$K_{2a} = K_{2s}\, dps(1-\varepsilon_{a0})/dpa(1-\varepsilon_{s0}) * (\varepsilon_{a0}-\varepsilon^*)/(\varepsilon_{s0}-\varepsilon^*) \quad (19)$$

$$D_{kia} = D_{kis}\, dps(1-\varepsilon_{a0})/dpa(1-\varepsilon_{s0}) \quad (20)$$

$$q_{1a} = q_{1s}\, dps(1-\varepsilon_{a0})/dpa(1-\varepsilon_{s0}) \quad (21)$$

$$q_{2a} = q_{2s}\, dps(1-\varepsilon_{a0})/dpa(1-\varepsilon_{s0}) \quad (22)$$

$$q_{bs} = q_{2s} \quad q_{ba} = q_{2a} \quad (23)$$

For the anthracite filter bed, little data was presented. When calculating the governing equations, it is important to reasonably assess the values of parameters, taking into account the difference in grain size. The filter run time for large grain filter beds is generally longer than that for small grain filter beds and the accumulation of deposits retained in former is greater than that the latter [5]. This indicates that grain size would affect not only the specific surface area and porosity of the filter bed but also the deposition rate, the detachment rate and the accumulation of deposits. Therefore, the deposition and detachment rates of particles and the mass of deposits saturated in the filter were evaluated taking into account the grain size as well as the porosity of the filter bed and were expressed as Eq. (18) to Eq. (22) shown in Table 2. In Table 2, K_{1s} and K_{2s} are the respective coefficients of Eq. (9)

and Eq. (10), and K_{1a} and K_{2a} are the respective coefficients of Eq. (7) and Eq. (8). D_{kis} and D_{kia} are detachment coefficients for the sand bed and the anthracite bed respectively. The values of operational parameters used in simulation are listed in Table 3.

ε_{a0} and ε_{s0} are the initial porosities of the anthracite and sand filter beds respectively, and ε^* is the ultimate porosity of the filter bed. It was assumed that ε^* did not change between the anthracite bed and the sand bed. The value of ε^* used in the present simulations was 0.279 [4].

3.4.4 Comparison with experiments

The solid lines in Fig.2 show the predicted residual deposits MR and dislodged mass MD as a function of the number of cycles. Although there is a small deviation between the predicted result and the experimental result, a good agreement has been achieved between the predicted result and the experimental data.

The solid line in Fig. 3 shows the predicted filtration effluent concentration profile. The predicted result shows the existence and characteristics of the initial degradation of filter effluent quality. Although there is a small deviation in the peak concentration and time between the predicted result and the experimental result, a good agreement has been achieved between the predicted result and the experimental data.

As far as the author is aware, there are no papers published for the simulation on an entire backwash process. However, simulation of the entire backwash process as well as the filtration process is essential to investigate the effect of the filtration/backwashing interaction. The solid line in Fig.4 shows the predicted backwash effluent concentration profile. The predicted result shows the characteristics of the backwash effluent concentration profile with time. Although there is a small deviation in the peak concentration and peak concentration time between the predicted result and the experimental result, the time concentration change of the backwash effluent has been well simulated by the model and the calculation method described in the previous section. These results show that the model presented for the sequence of filtration and backwash cycles described in the previous section could capture the effect of interaction between filtration and backwash cycles and should be able to predict filter performance when the model parameters are determined for a particular filtration system.

Table 3 Values of kinetic and operational parameters used in the model

Filtration	140 m/h	
q_{1s} (kg/m^3)	0.121	
q_{1a}(kg/m^3)	0.051	
q_{2s}(kg/m^3)	10.1	
q_{2a}(kg/m^3)	23.8	
K_{1s}(1/h)	5.0	
K_{1a}(1/h)	2.12	
K_{2s}(1/h)	16.0	
K_{2a}(1/h)	16.2	
D_{bs} (m^2/h)	0.125	
D_{ba} (m^2/h)	0.22	
Backwash	36 m/h	54 m/h
Fixed stage		
D_{kFs} (1/h)	28.8	86
D_{bFs} (m^2/h)	0.12	0.252
D_{bFa}(m^2/h)	0.12	0.252
D_{bFf} (m^2/h)	0.225	0.504
Violent stage		
Quick ejection (sec)	10	5
D_{kRs} (1/h)	173	389
D_{bRs}(m^2/h)	18	45.4
D_{bRa} (m^2/h)	22.5	55.4
D_{bRf} (m^2/h)	22.5	55.4
Turbulence (sec)	40	40
D_{kTs}(1/h)	116	260
D_{bTs}(m^2/h)	0.18	0.554
D_{bTa} (m^2/h)	0.25	0.71
(m2/h)	0.54	1.15
Stabilized stage (sec)	146	102
D_{kSs} (1/h)	57	260
D_{kSs} (m^2/h)	0.18	0.378
D_{bSs} (m^2/h)	0.224	0.403
D_{bSa} (m^2/h)	0.45	0.506

3.4.5 Impact of the residual deposit on the optimum filtration operation

Although the filter ripening stage will inevitably occur in the first cycle of successive operations of filtration and backwash, it may be eliminated in other cycles. This is because the filter ripening stage does not occur once the amount of residual deposits reaches a threshold. Therefore, operating conditions were investigated based on the

amount of residual deposits. As shown in Fig. 2 deposits remained in filter beds increase with the number of cycles, N. If the amount of deposit reaches the threshold in the first cycle, the amount of residual deposits in subsequent cycles will be greater than that. Hence, the operating conditions may be determined by whether the ripening stage appears at the second cycle of successive operations of filtration and backwash.

The two-stage backwash method would be one effective backwash method to control the filter ripening stage. The effect of the two-stage backwash method on the control of filter ripening stage was investigated by using the model described in the previous section. The two-stage backwash method consists of the conventional backwash (first stage backwash) and the second stage backwash following the first stage with specific conditions of backwash flow rate and backwash duration. Based on the literature [10], the second stage backwash flow rate was set to 21 m/h and the second stage backwash period was set to the retention time of the water flow through the filter. D_k, D_{bs}, D_{ba} and D_{bf} were also taken from the literature [10,22] and set as follows: D_k =0.158 (1/h), D_{bs} =0.18 (m^2/h), D_{ba}=0.225 (m^2/h), D_{bf}=0.405 (m^2/h).

In Fig.3, Two-stage backwash 1, shows the predicted filter effluent concentration profile based on the two-stage backwash method which consists of the conventional backwash (first stage) and the specified second stage. Although the peak concentration of filter effluent significantly decreased, the quality of the filter effluent deteriorates in the beginning stages of filtration. This shows that conventional backwash duration in the first stage is likely to result in over-efficient cleaning. However, in a 1.5 m deep filter bed, no filter ripening stage was observed even with a two-stage backwash method consisting of a conventional backwash (first stage) and a specified second stage [9]. These results suggest that the threshold of residual deposits would be affected by characteristics of the filter bed such as filter layer thickness and filter media composition.

In anticipation of increasing residual deposits, the effect of the first stage backwash duration on the control of filter ripening stage was investigated under the same conditions of filtration rate, backwash flow rate, second stage backwash duration, etc. As shown in Fig.3, Two-stage backwash 2, the predicted filtration effluent concentration is well below 0.1 mg/L, and no filter ripening stage appears. Similarly, no filter ripening stage appeared during the filtration process of other cycles. As shown by the dotted line in Fig.2, the predicted MR increased by decreasing the first stage backwash duration to 75 seconds. The predicted average residual deposits concentration in the filter bed after backwashing was approximately 2.5 times higher than that of Two-stage backwash 1, and the predicted average residual suspended solids concentration was approximately 1/20 of that of Two-stage backwash 1. In the calculations using this model, no filter ripening stage appeared in the filter process by setting the first stage backwash duration in the range of 90 seconds with a minimum of approximately 60 seconds that results in the peak concentration of the backwash effluent. The time to peak concentration of the backwash effluent would be an indicator of effective backwash duration.

However, simulated results for the backwash rate of 54m/h showed that the filter ripening stage could not always be eliminated for the filter layer thickness of 0.6 m even by the specified two-stage backwash method which corresponds to the two-stage backwash 2; the backwash flow rate of 54m/h would be too fast to maintain the required amount of residual deposits.

IV. CONCLUSION

The characteristics of the sequence of filtration and backwash cycles with particular emphasis on the effect of filtration/backwash interaction, were analyzed with the phenomenological model based on quantitative results related to filtration and backwashing. The following conclusions are drawn.

1. The conventional backwash duration is likely to result in over- efficient cleaning. Decreasing the backwash duration increases deposits retained in the filter bed, and the increased residual deposits will be beneficial for controlling the ripening stage.
2. There is a threshold of residual deposits to eliminate the filter ripening stage in successive

operations of filtration and backwash. The threshold will be affected by the characteristics of filter beds.

3. The operating conditions predicted based on residual deposits will be appropriately apply not only for controlling the filter ripening stage, but also for truly evaluating filtration operations. The amount of residual deposits would be a relevant basic condition for an optimum filtration and the time to peak concentration of the backwash effluent would be an indicator of effective backwash duration.
4. Most of the solids deposited in the filtration are removed by the backwash water ejected from the filter bed at the beginning of the backwash (backwash water jet).

Acknowledgements

The paper incorporates experimental data collected by E. Ohata and A. Yoshida at the Yamato Corporation Environmental Technology Research Center, whose contribution is gratefully acknowledged.

REFERENCES

[1]. H. Noguchi, T. Ueda, On the mechanism of filter backwashing. *Proceeding of the Japan Society of Civil Engineers*, *1978 Issue 272,* 1978,39-51.

[2]. RI. Mackie, RMW. Horne, RJ. Javis, Dynamic modeling of deep-bed filtration. *AIChE J.*,*33*, 1987,1761-1775.

[3]. BH. Bhargava, CSP. Ojha, Theoretical analysis of the backwash time in rapid gravity sand filters. *Wat. Res*., *23,* 1989, 581-587.

[4]. S. Vigneswaran, JS. Chang, Experimental testing of mathematical models describing the entire cycle of filtration. *Wat. Res.*, *23*, 1989, 1413-1421.

[5]. H. Hozumi, H. Yoshida, M. Jarahn, H. Ioroi, A study of advanced treatment of secondary wastewater effluent by a dual media filter-Effect of filtration rate on filter performance. *Proceeding of Environmental Engineering Research,* 1995, 339-347.

[6]. J. Jegatheesan, S. Vigeneswaran, Deep bed filtration: Mathematical models and observations. *Critical reviews in Environmental Science and Technology*, *35,* 2005, 515-569.

[7]. A. Amirtharajah, DP. Westin, Initial degradation of filter effluent quality during filtration. *J. AWWA*., *72* **,**1980, 518-524.

[8]. A. Amirtharajah, The interface between filtration and backwashing. *Wat. Res*., *5* ,1985, 581-588.

[9]. JF. Colton, P. Hills, CSB. Fitzpatrick, Filter backwash and startup strategy for enhanced particulate removal. *Wat. Res*.,*30(10)* ,1996, 2502-2507.

[10]. JE. Amburgey. Optimization of the extended terminal subfluidization wash (ETSW) filter backwashing procedure. *Wat. Res.*, *39***,** 2005, 314-330.

[11]. BM. Brouckaert, A. Amirtharajah, CJ. Broucmaert, JE. Amburgey, Predicting the efficiency of deposit removal during filter backwash. *Water SA*., *32(5)*, 2006, 633-640.

[12]. SJ. Han, CSB. Fitzpatric, A. Wetherill, Simulation on combined rapid gravity filtration and backwash models. *Water Science & Technology*, *59(12),* 2009, 2429-2435.

[13]. CR. O'Melia, W. Ali, The role of retained particles in deep bed filtration. *Progress Water Technology*, *10*, 1978, 167-182.

[14]. A. Cescon, JQ. Jiang, Filtration and alternative filter media material in water treatment. *Water*, *12*, 2020, 3377 1-20.

[15]. AC. Payatakes, HY. Park, J. Petrie, A visual study of particle deposition and re-entrainment during depth filtration of hydrosols with a polyelectrolyte. *Chem. Eng. Sci., 36***,** 1981, 1319-1335.

[16]. CSP. Ojha, NJD. Graham, Theoretical estimates of bulk specific deposit in deep bed filters. *Water Res., 27***,** 1993, 377-387.

[17]. V. Gitis, I. Rubinstein, M. Livshits, G. Ziskind, Deep-bed filtration model with multistage deposition kinetics. *Chemical Engineering J.*,*163*, 2010, 78-85.

[18]. T. Iwasaki, Some notes on sand filtration. *J. of American Water Works Association*, *29(5),* 1937, 1591-1602.

[19]. KJ. Ives, Rapid filtration. *Wat. Res*., *4***,** 1970, 201-223.

[20]. C. Tien, AC. Payatakes, Advances in deep bed Filtration. *AIChE J*., *25*, 1979,737-759.

[21]. K. Kubo, T. Aratani, A. Mishima, Axial mixing characteristics in packed bed-Analysis based on side mixing model. *Kagakukogaku Ronbunshu*, *7(3)*, 1981, 304-308[in Japanese with English abstract].

[22]. K. Kikuchi, S. Kakutani, T. Sugawara, H. Ohashi, Axial dispersion of liquid in liquid fluidized beds in the low Reynolds number region. *J. Chemical Engineering Japan*, *17*, 1984, 362-367.

[23]. K. Wojciechowska, Modeling and simulation of filtration in the development of water treatment technology. *Engng. Trans*., *50(4)*, 2002, 323-357.